Brain, Behavior, and Immunity 112 (2023) 29–41

Contents lists available at ScienceDirect

Brain Behavior and Immunity

journal homepage: www.elsevier.com/locate/ybrbi

Full-length Article

Zika Virus affects neurobehavioral development, and causes oxidative stress associated to blood–brain barrier disruption in a rat model of congenital infection

Wellington de Almeida [a,b], Bruna Ferrary Deniz [c], Adriana Souza dos Santos [a,b], Aline Martins Faustino [b], Osmar Vieira Ramires Junior [d], Felipe Schmitz [d], Ana Paula Muterle Varela [e], Thais Fumaco Teixeira [e], Patrícia Sesterheim [f,g], Fernanda Marques da Silva [f], Paulo Michel Roehe [e], Angela TS. Wyse [d], Lenir Orlandi Pereira [a,b,*]

[a] Programa de Pós-Graduação em Neurociências, Instituto de Ciências Básicas da Saúde, Universidade Federal do Rio Grande do Sul, Porto Alegre, RS, Brazil
[b] Departamento de Ciências Morfológicas, Instituto de Ciências Básicas da Saúde, Universidade Federal do Rio Grande do Sul, Porto Alegre, RS, Brazil
[c] Departamento de Fisiologia e Farmacologia, Instituto de Biologia, Universidade Federal de Pelotas, Pelotas, RS, Brazil
[d] Laboratório de Neuroproteção e Doenças Neurometabólicas, Departamento de Bioquímica, Instituto de Ciências Básicas da Saúde, Universidade Federal do Rio Grande do Sul, Porto Alegre, RS, Brazil
[e] Laboratório de Virologia, Departamento de Microbiologia Imunologia e Parasitologia, Instituto de Ciências Básicas da Saúde, Universidade Federal do Rio Grande do Sul, Porto Alegre, RS, Brazil
[f] Programa de Pós-Graduação em Ciências da Saúde: Cardiologia, Instituto de Cardiologia/Fundação Universitária de Cardiologia, Porto Alegre, RS, Brazil
[g] Centro de Desenvolvimento Científico e Tecnológico, Centro Estadual de Vigilância em Saúde da Secretaria de Saúde do Estado do Rio Grande do Sul, Porto Alegre, RS, Brazil

ARTICLE INFO

Keywords:
Zika virus
Neurodevelopmental outcomes
Neonatal disabilities
Neurobehavioral assessments
Blood–brain barrier
Oxidative stress
Congenital zika virus infection
Neurobehavioral development

ABSTRACT

Zika virus (ZIKV) is a mosquito-borne *flavivirus* associated with several neurodevelopmental outcomes after *in utero* infection. Here, we studied a congenital ZIKV infection model with immunocompetent *Wistar* rats, able to predict disabilities and that could pave the way for proposing new effective therapies. We identified neurodevelopmental milestones disabilities in congenital ZIKV animals. Also, on 22nd postnatal day (PND), blood–brain barrier (BBB) proteins disturbances were detected in the hippocampus with immunocontent reduction of β_Catenin, Occludin and Conexin-43. Besides, oxidative stress imbalance on hippocampus and cortex were identified, without neuronal reduction in these structures. In conclusion, even without pups' microcephaly-like phenotype, congenital ZIKV infection resulted in neurobehavioral dysfunction associated with BBB and oxidative stress disturbances in young rats. Therefore, our findings highlighted the multiple impact of the congenital ZIKV infection on the neurodevelopment, which reinforces the continuity of studies to understand the spectrum of this impairment and to provide support to future treatment development for patients affected by congenital ZIKV.

1. Introduction

Zika virus (ZIKV) is an arbovirus classified into the family *flaviviridae,* genus *flavivirus,* which was responsible for an important epidemic in the Americas in 2015 (Song et al., 2017). Gestational ZIKV infection was soon associated with neurodevelopmental outcomes of fetuses and a range of damages were observed such as intrauterine growth restriction, fetal death and consequent miscarriage, stillbirth, and eyes disorders (Alvarado and Schwartz, 2017; Coyne and Lazear, 2016). Among them, microcephaly was the most evident change observed and today is known to be associated with vertical transmission of ZIKV (Wang & Ling, 2016; Li et al., 2016). Despite assuming that microcephaly would be the major infection-induced neurological consequence, recent studies have shown that neurodevelopmental delays can be observed in children who are victims of congenital ZIKV infection without microcephaly (Sobral da Silva et al., 2021). Nevertheless, it is becoming increasingly clear that the ZIKV pathogenicity is not restricted to the damage observed shortly after birth and there is convincing evidence of long-term impacts.

* Corresponding author at: Programa de Pós-Graduação em Neurociências. Departamento de Ciências Morfológicas. Universidade Federal do Rio Grande do Sul., Rua Sarmento Leite, 500, 90050-170 Porto Alegre, RS, Brazil.
E-mail addresses: bruna.deniz@ufpel.edu.br (B.F. Deniz), wyse@ufrgs.br (A.TS. Wyse), lenir_pereira@yahoo.com.br, lenir.orlandi@ufrgs.br (L.O. Pereira).

https://doi.org/10.1016/j.bbi.2023.04.014
Received 8 September 2022; Received in revised form 16 March 2023; Accepted 30 April 2023
Available online 3 May 2023

Several models have been proposed to understand the pathophysiology of infection and its relationship with neurological damage. *In vitro* studies have been carried out to assess how viral infection can lead to cell function changes and to trigger the observed consequences. A study used U87-MG and HepG2 cells (human glioblastoma and human liver carcinoma cell line, respectively) verified that Zika virus infected cells had reactive oxygen species, lipid peroxidation, and protein carbonylation products increase, in addition to decreased superoxide dismutase and catalase activities (Almeida et al., 2020). Human neural progenitor cells (hNPCs) infected revealed cell cycle dysregulation and caspase 3 increase culminating with cell death (Tang et al., 2016). Disrupted mitosis and structural disorganization also can be verified in radial glial cells (RGCs); ZIKV infection can also, during mitosis, cause sequestration of phospho-TBK1 in RGCs (Onorati et al., 2016). Since RGC's are important for cortical cell migration, the above data are useful to explain the findings concerning the cortical thickness reduction consequent to ZIKV infection.

Another important damage identified after ZIKV infection occurs in the blood–brain barrier (BBB), an important protective barrier between systemic circulation and nervous parenchyma (Clé et al., 2020). BBB integrity disturbance caused by infection was observed *in vitro* and *in vivo* experiments (Leda et al., 2019). However, it is unclear whether these changes are only transient or can also be lasting, as well as it is not completely understood the myriad of damage caused by infection on this structure.

Considering *in vivo* studies, several rodent models have been used to evaluate ZIKV pathogenicity, fetal infection and vertical transmission using rodents as models. Due to the difficulty in using Wild-Type (WT) rodents for accessing ZIKV infection consequences, many studies have been proposed with animals' interferon (IFN)-deficient, since ZIKV has difficulty in face up to IFN produced by rodents (Kublin and Whitney, 2018). Such studies with immunosuppressed animals, as mice A129 and AG129, were crucial in elucidating vertical transmission impact (Vue and Tang, 2021). Many other proposed animal models have adopted different infection routes, such as intrauterine infection directly in the developing rodents' brain (Li et al., 2016), or animals are infected just after birth (Lazear et al., 2016; Miner et al., 2016). It is clear the demand for the development of more studies with immunocompetent animals, which is essential for understanding the immune response establishment, the long-term disabilities and for testing developing vaccines and treatments (Morrison & Diamond, 2017).

In a study with immunocompetent mice, retrobulbar ZIKV infection in pregnant females did not cause obvious phenotypes at the pup's birth but promoted an increase in the number of immature neurons in the hippocampus. Males also showed increased testosterone levels associated with impaired learning and memory (Stanelle-Bertram et al., 2018). This interesting study draws attention to long-term deficits even without obvious phenotypes at birth. Another rat model has been proposed by performing viral inoculation in immunocompetent pregnant females. Sherer and coworkers have performed virus inoculation in pregnant rats on 18th embryonic day (E18) (Sherer et al., 2019). In that study, neonatal cell death and cortical/hippocampal atrophy were identified. More recently, they reported that prenatal infection on E18 produced transitory increase and decrease area in some hippocampus regions, showing altered developmental trajectory in neonatal brains (Patel et al., 2021). Using the same animal model, motor alterations were identified, when evaluated in adulthood, indicating long-term disturbances (Sherer et al., 2021). Neurodevelopmental assessments after ZIKV infection are of great value since they are predictors of neurological changes, as seen in humans (El-Dib et al., 2012); there is another recent study reporting that long-term changes can be observed in ZIKV infection models (Snyder-Keller et al., 2019).

Considering that the neurodevelopmental impact of gestational ZIKV infection is not yet clarified and seeking to contribute to the progress of studies in this area, our research group has been developing an immunocompetent rat model of congenital infection more reliable for understanding the neurobiology of congenital syndrome of ZIKV in humans. For this, we have proposed a rat model with infection performed in E9, a critical period for the nervous system development, when the neural tube closure occurs in rodents, triggering an intense neurogenesis period (Jacobson et al., 1999; Kim et al., 2011). We sought to evaluate pup rats' development through neurobehavioral assessments analyses and, aiming to observe possible pathological associated findings, we evaluated BBB changes, tissue redox status and neuronal density in the hippocampus and cortex.

2. Methods

The investigators were not blinded to allocation during animal procedures due to the biological safety care.

2.1. Viral culture and amplification

The ZIKV strain 17 (ZIKV 17), isolated from Brazilian patient (Oliveira et al., 2018), was propagated in Vero cells (ATCC CRL-1586) and were kept at −80∘C until use. Viral quantification was determined by standard plaque-forming assays.

2.2. Animal procedures

Pregnant female *Wistar* rats, approximately two months old, from the Animal Reproduction and Experimental Center of the Federal University of Rio Grande do Sul, Brazil, were used. The animals were kept in individually ventilated cages (IVC), 12 h light / dark cycle, with controlled temperature (21 ± 2° C) and with free access to water and food. All adopted procedures were carried out in accordance with the ethical principles recommended by the National Council for Animal Experimentation of Brazil and Brazilian law for procedures and scientific use of animals (11.794/08), as well the Guide for the Care and Use of Laboratory Animals of the National Research Council - USA ("Guide for the Care and Use of Laboratory Animals," 2011).

Ethical approval for this study was obtained from the Ethics Committee of the Federal University of Rio Grande do Sul (approval number 33452/2017). All procedures were performed in a BSL-2 laboratory, under Animal Biosafety Level 2 precautions, in accordance with Center for Disease Control and Prevention (CDC) recommendations for laboratory procedures with Zika virus. Procedures with virus manipulation and animals were carried out in a Class II Biological Safety Cabinet (BSC) (Tecniplast® BS 60 class II, Buguggiate, Italy).

At the 9th embryonic day (E9), pregnant females were separated in two groups: five females inoculated with intraperitoneal injection 500 µl of 1×10^6 plaque-forming unit (PFU mL^{-1}) of Zika virus isolated in Brazil ($ZIKV^{BR}$) and six females inoculated with 500 µl intraperitoneal injection of sterile diluted medium (Fig. 1).

Six hours after inoculation a blood collection was made in a caudal vein of the rats for confirmation of the infection through Quantitative Polymerase Chain Reaction (qPCR) analysis. After these procedures, animals were kept in the IVC's and were observed daily until the end of gestation. To verify the animals health condition, sickness behavior, such as piloerection, curled up posture, and signs of pain were observed daily by researchers and veterinarians after ZIKV infection.

2.3. RNA extraction and qPCR analysis

Total RNA was isolated from maternal blood six hours after inoculation using TRIzol™ Ambion™ (Thermo Fisher Scientific, Waltham, MA, USA), according to manufacturer's instructions. RNA was submitted to cDNA synthesis by High-Capacity cDNA Reverse Transcription Kit (Applied biosystems, Thermo Fisher Scientific, Waltham, MA, USA) following to ZIKV quantitative PCR (Lanciotti et al., 2008; Wachholz et al., 2021). The reactions were carried out in the Step OneTM Real-Time PCR system (Applied biosystems, Thermo Fisher Scientific,

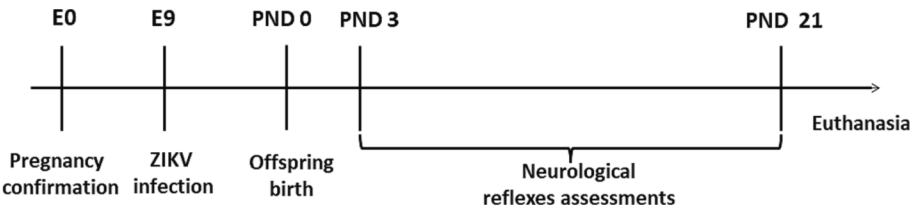

Fig. 1. Representative timeline of experimental procedures. (E0) embryonic day 0. (E9) 9th embryonic day. (PND 0) postnatal day 0. (PND 3) 3rd postnatal day. (PND 21) 21st postnatal day.

Waltham, MA, USA) under conditions previously described by Wachholz et al. (2021).

Twenty-four hours after infection samples of the spleen and uterine horns of three ZIKV pregnant rats and three fetuses of each dam were used for viral detection and quantification. Viral titer was determined by the standard Plaque Assay method, after this total RNA extracted from infected culture supernatants was analyzed for the number of ZIKV genomes by RT-PCR using the One-Step RT-ddPCR kit (Bio-Rad, Hercules, CA), adapted from Dangsagul et al. (2021) (details in supplementary material).

2.4. Neurological reflexes

Twenty-four hours after birth, standardization of litters (5–8 puppies by litter) and body measurements (Table 1) were performed. To investigate neurodevelopmental impairments resulting from gestational Zika virus infection the evaluation of neurological reflexes was realized. This evaluation started on PND 3 and was held every three days until PND 21. The assessment consisted of observing the physical characteristics such as weight, eye opening and incisor tooth eruption (Lubics et al., 2005). Also were evaluated the *Righting reflex*: animals were placed with their back on the surface and the time until they returned to a prone position and keep their four paws in contact with the surface was recorded. *Negative geotaxis*: rats were placed on an inclined platform (45°) with their heads facing down. It was noted the day when the animals could turn their heads up and climb the platform, the maximum time to perform the task was 30 s. *Limb placing*: the posterior region of the animal's forepaw and hind paw was leaning against a surface and the day that the animal placed the paws on the surface was recorded. *Limb grasp*: the back of forelimb paws was touched on a stem and the day the animals grasped the stem was noted. *Cliff aversion*: animals were placed with their heads on the edge of an elevated platform and the time taken to turn their heads in the opposite direction was registered as well as the first day that they presented this behavior. *Gait*: rats were placed in the center of a circle with 30 cm of diameter and the time they took to leave the circle was observed as well as the day they began to move. *Homing behavior*: On one side of a clean box was placed bedding of the homing box and on the other side the same amount of sterile fresh bedding. The animals were placed on the midline between the two and the time to reach the chosen side was considered as well as the wrong choices. The maximum time to perform the test was 300 s (Deniz et al., 2018; Lubics et al., 2005; Sanches et al., 2012). Female CT (n = 8); Female ZKV (n = 7); Male CT (n = 15); Male ZKV (n = 15).

Table 1
Body measurements of pups 24 h after birth. Data are expressed as mean ± SEM. (ZKV) animals that had their mothers infected with the *Zika* virus during pregnancy. (CT) Animals of the control group. Female CT (n = 8); Female ZKV (n = 7); Male CT (n = 15); Male ZKV (n = 15). *Two-way* ANOVA. No difference was found in the performed analyzes.

Body measurements of pups	Total length	Tail length	Head width	Head length
Female CT	50.57 ± 0.57	18.14 ± 0.42	9.92 ± 0.21	17.85 ± 0.31
Female ZKV	51.00 ± 0.57	18.28 ± 0.42	10.07 ± 0.21	18.00 ± 0.31
Male CT	51.25 ± 0.37	17.81 ± 0.27	10.15 ± 0.13	17.93 ± 0.20
Male ZKV	51.63 ± 0.57	18.20 ± 0.28	10.30 ± 0.14	18.20 ± 0.21

2.5. Tissue collection

Part of the animals from both experimental groups were anesthetized with Ketamine (90 mg/kg) and Xylazine (10 mg/kg) i.p. and transcardiac perfused with 0.9% saline solution followed by fixation solution (4% paraformaldehyde in 0.1 M phosphate buffer, pH 7.4). Subsequently, brains were removed, post-fixed in the same fixative solution, cryoprotected in 30% sucrose, frozen and stored at −80 °C until analysis. Part of the brains collected was post-fixated in 4% paraformaldehyde /2,5% glutaraldehyde *overnight,* for morphological analysis.

For protein immunodetection and oxidative stress analysis, animals from both groups that have not performed behavioral tests were decapitated using a guillotine. Soon after decapitation, brains were removed, cortex and hippocampus were dissected, collected, and stored at −80 °C.

2.6. Protein immunodetection

Protein immunodetection and quantification was performed by western blotting (WB) analysis. PND 22 animals had their brains removed and hippocampus and cortex were isolated. Samples were homogenized with extraction cocktail, centrifuged (3000gx10min) and supernatants were used to blotting analysis and total protein quantification by Bradford method, using Bovine Serum Albumin (BSA) as standard (Kielkopf et al., 2020).

The WB protocol used in our study followed previously published studies. Briefly, proteins were resolved on SDS PAGE gel and transferred to PVDF membrane. Then, membranes were incubated with BSA 3%, washing in TBS-T and incubated with the following primary antibodies: aquaporin 4 (1:1000; sc-32739), β-catenin (1:500; sc-7963), connexin 43 (1:500; sc-271837), GFAP (1:100; sc-33673), GLUT-1 (1:500; sc-7903), occludin (1:500; sc-133256), all of them from Santa Cruz Biotechnology (Santa Cruz, CA, USA). After this, membranes were washed in TBS-T and incubated with secondary antibody conjugated with horseradish peroxidase (HRP) anti-mouse for aquaporin 4, β-catenin, connexin 43, GFAP and occludin, and anti-rabbit for GLUT-1 antibody. Then, membranes were stripped and incubated with β-tubulin (1:10.000; T4026, Sigma, St. Louis, MO, USA.) for internal control (Diaz et al., 2016). Membranes were revealed in Invitrogen™ iBright™ Imaging System (Thermo Fisher Scientific, Waltham, MA, USA) and imagens were analyzed using Image J 1.53e Software (NIH, Bethesda, MD, USA). Data is shown as a percentage of control. CT (n = 7); ZKV (n = 6).

2.7. Redox status evaluation

Samples from the cortex and hippocampus on PND 22 were homogenized with extraction cocktail, centrifuged (1000gx10min) and supernatants were gathered and used to following analysis: 2′,7′-Dichlorofluorescein (DCF), Sulfhydryl content, Thiobarbituric acid-reactive substances (TBARS), Superoxide dismutase (SOD) activity and Catalase (CAT) activity. These markers were analyzed according to

protocols previously described (Sasso et al., 2015; Schweinberger et al., 2015). Briefly, for DCF analysis the fluorescent compound produced by 2′,7′-dichlorofluorescein diacetate cleavage (oxidized by reactive species present in the samples) was quantified using 488 nm excitation and 525 nm emission. Results are expressed as nmol DCF / mg protein. For TBARS analysis, samples were incubated with trichloroacetic acid and thiobarbituric acid in a hot water bath. TBARS was quantified by measuring the absorbance at 535 nm. 1,1,3,3-tetramethoxypropane was used as the standard calibration curve and results were expressed as nmol TBARS / mg protein. Sulfhydryl content analysis was made with incubation of samples and Ellman's reagent 5,5́-dithiobis (2- nitrobenzoic acid) (DTNB). Absorbance at 412 nm was made to determinate total sulfhydryl content. Results are described as nmol thionitrobenzoic acid (TNB) / mg protein. SOD activity was performed using pyrogallol autoxidize process based. Pyrogallol was added in samples and absorbance was recorded at 420 nm. SOD purified was used as standard to calculate SOD activity. Total SOD required to inhibit 50% of pyrogallol autoxidation is considered SOD unit. Results are expressed as SOD unit / mg protein. CAT assay is centered on decomposition of peroxide hydrogen (H_2O_2) in a reaction medium buffered with 01–03 mg protein/ml. One μmol of H_2O_2 consumed per minute is described as CAT unit. CAT activity is determined as CAT units/mg protein. CT (n = 7); ZKV (n = 6).

2.8. Morphological analysis

For morphological analysis, the brains' coronal sections were performed. Semi-thin sections (1 μm) were obtained using an ultramicrotome (Power Tome X, RMC, Tucson, USA) and stained with toluidine blue. The images were analyzed on microscopy (Zeiss Axio Imager M2) coupled to a digital camera (Zeiss, AxioCam MRc, Oberkochen, Baden-Württemberg, Germany). Neurons of the CA1 region of the hippocampus were counted using a 630-fold increase. Cortical neurons were also counted at an increase of 630 times. Five cuts of the brain per animal were used, and two regions were analyzed in each section. Hippocampus CT (n = 3); ZKV (n = 3). Cortex CT (n = 4); ZKV (n = 4).

2.9. Statistical analysis

Two-way ANOVA was performed to compare male ZKV with male CT and female ZKV with female CT for pup's body measurements (total length, tail length, head length and head width). One-way repeated-measures ANOVA and general linear model (GLM) for repeated measures followed by Tukey's *post hoc,* when required, was employed for evaluating the following variables: aversion to fall, gait, negative geotaxis, homing behavior and righting reflex. Additional Student *t*-test was executed for each day when appropriated. This test was also used for Neurological reflexes' day of appearance, comparing male ZKV with male CT and female ZKV with female CT. For histological analysis, protein immunodetection and redox status evaluation Student *t*-test or Wilcoxon-Mann-Whitney test was performed according to normality test results.

3. Results

3.1. Viral quantification after qPCR analysis

After quantification of total RNA isolated from maternal blood six hours after infection the following amounts of viral copies were identified in infected females: $4{,}6x10^3$; $1{,}2x10^4$, $1{,}3x10^4$, $2{,}2x10^4$, $1{,}9x10^3$, confirming the virus presence after infection.

Plaque assay analyses realized twenty-four hours after infection showed 25 % of cytopathic effect (CPE) on spleen and uterine horns of the pregnant rats and 50% of cytopathic effect on fetuses (supplementary table and Fig. 1). Viral presence was identified on spleen (1,8x10 PFU), uterine horns (10^4 PFU) and fetuses ($1{,}2x10^4$ PFU), indicating active viral replication (supplementary Fig. 2).

3.2. Body measurements of pups

Two-way ANOVA was performed to compare male and female ZKV with male and female CT for the total length, tail length, head length and head width. No differences were found in total length (*group* (F (1,41) = 0.69, p = 0.40), *sex* (F (1,41) = 1.81, p = 0.18) and *group*sex* interaction (F(1,41) = 0.00, p = 0.96)), tail length (*group* (F (1,41) = 0.54, p = 0.46), *sex* (F (1,41) = 0.33, p = 0.56) and *group*sex* interaction (F(1,41) = 0.12, p = 0.73)), head length (*group* (F (1,41) = 0.59, p = 0.44), *sex* (F (1,41) = 0.28, p = 0.59) and *group*sex* interaction (F(1,41) = 0.05, p = 0.82)), or head width (*group* (F (1,41) = 0.54, p = 0.42), *sex* (F (1,41) = 1.62, p = 0.21) and *group*sex* interaction (F(1,41) = 0.00, p = 0.99)) (Table 1).

3.3. Day of appearance of the neurological reflexes

For the evaluation of neurological reflexes, *t*-test was used comparing male ZKV with male CT and also comparing female ZKV with female CT. Significant difference indicating delay in neurological reflexes expression was found comparing male ZKV to male CT in the following variables: Incisor tooth eruption (t(28) = 5.82; P < 0.05), Forelimb placing (right) (t(28) = 4.58; P < 0.05), Hind limb placing (right) (t(28) = 5.15; P < 0.05), Hind limb placing (left) (t(28) = 3.35; P < 0.05), Forelimb grasp (right) (t(28) = 2.15; P < 0.05). No differences were found in the day of appearance of the Eye opening, Negative geotaxis, Forelimb placing (left), Forelimb grasp (left), Gait, Aversion to fall, Righting Reflex and Olfactory behavior (Table 2). For female, the same analysis was performed and delay in appearance reflexes was also identified in the following variables: Hind limb placing (right) (t(13) = 3.10; P < 0.05), Hind limb placing (left) (t(13) = 4.56; P < 0.05) and Righting Reflex (t(28) = 2.28; P < 0.05). No differences were found in the other analysis

Table 2
Analysis of the day of appearance of the neurological reflexes. Data are expressed as mean ± SD. (ZKV) animals that had their mothers infected with the *Zika* virus during pregnancy. (CT) Animals of the control group. Female CT (n = 8); Female ZKV (n = 7); Male CT (n = 15); Male ZKV (n = 15). * Represents difference when compared to CT group of the same sex. Student's *t*-test. p < 0.05.

Neurological reflexes – Day of appearance	Female CT	Female ZKV	Male CT	Male ZKV
Eye opening	15.3 ± 1.06	15.00 ± 0.00	15.40 ± 1.05	15.00 ± 0.00
Incisor tooth eruption	9.37 ± 1.06	9.85 ± 1.46	9.60 ± 1.24	11.80 ± 0.77*
Negative geotaxis	10.12 ± 1.55	9.42 ± 2.07	9.20 ± 1.78	9.20 ± 1.78
Forelimb placing (right)	3.00 ± 0.00	3.85 ± 1.46	3.00 ± 0.00	4.80 ± 1.52*
Forelimb placing (left)	3.37 ± 1.06	3.85 ± 1.46	3.80 ± 1.78	4.40 ± 1.54
Hind limb placing (right)	4.50 ± 1.60	8.14 ± 2.85*	4.40 ± 1.91	8.20 ± 2.11*
Hind limb placing (left)	4.87 ± 1.55	10.28 ± 2.92*	5.00 ± 2.44	8.00 ± 2.44*
Forelimb grasp (right)	5.25 ± 2.12	5.14 ± 2.85	5.40 ± 2.58	7.40 ± 2.50*
Forelimb grasp (left)	6.00 ± 2.26	4.28 ± 2.36	5.60 ± 2.50	7.40 ± 2.50
Gait	6.37 ± 3.73	9.00 ± 3.00	8.00 ± 3.13	7.20 ± 2.48
Cliff aversion	9.75 ± 2.12	9.85 ± 2.26	8.40 ± 2.58	7.20 ± 1.89
Righting Reflex	3.00 ± 0.00	4.28 ± 1.60*	3.00 ± 0.00	3.20 ± 0.77
Homing behavior	6.37 ± 2.50	8.57 ± 3.20	6.40 ± 3.18	8.00 ± 2.69

performed (Table 2). Together, these results on males and females reveal a delay in the day of appearance of some neurological reflexes, indicating consequences from gestational infection caused by the Zika virus that can be predictive of future neurologic changes in offspring.

3.4. Cliff aversion

One-way repeated-measures ANOVA followed by Tukey's test when necessary was performed for each sex comparing ZKV with CT in aversion to fall, gait, negative geotaxis, homing behavior and righting reflex. In cliff aversion reflex, no differences were found for the factor *group* when compared male ZKV to male CT ($F(1,28) = 0.30$, $p = 0.58$). *Day* factor presents a significant effect ($F(5,140) = 142.89$, $p = 0.00$), showing reduction in latency over time. When compared female ZKV to CT no differences were found for factor *group* ($F(1,13) = 0.11$, $p = 0.74$); on the other hand, as expected, *Day* factor resulted in significative difference ($F(5,65) = 74.43$, $p = 0.00$), indicating evolution in the task execution over the days (Table 3). Repeated measures GLM analysis did not reveal significant differences for factors *group* ($F(1,42) = 0.07$, $p = 0.77$) or *sex* ($F(1,42) = 0.68$, $p = 0.41$). There are also no significant differences between *group*day* interaction ($F(5,210) = 0.31$, $p = 0.90$) or *sex*day* ($F(5,210) = 1.90$, $p = 0.09$).

3.5. Gait

One-way repeated-measures ANOVA general result of the gait not show differences for *group* factor when compared male ZKV to male CT ($F(1,28) = 4.84$, $p = 0.036$), however, showed significant result specifically on PND15 ($F(1,28) = 1.03$, $p = 0.31$), evidencing ZKV delay on this day. *Day* factor presents a significant difference ($F(6,168) = 182.42$, $p = 0.00$), showing reduction in latency over time for both groups, as expected. One-way repeated-measures ANOVA compared female ZKV to female CT not show difference for *groups* ($F(1,13) = 0.41$, $p = 0.53$), however, there were *day* ($F(6,78) = 69,84$, $p = 0.00$) and *group*day* ($F(6,78) = 2.49$, $p = 0.02$) interaction effects. Nonetheless, Tukey *post-hoc* did not show any significant difference. Complementary GLM repeated measures analysis did not show differences for factor *group* ($F(1,42) = 1.48$, $p = 0.23$) or *sex* ($F(1,42) = 0.00$, $p = 0.96$) factors. There were also no significant differences between *day* ($F(6,252) = 0.21$, $p = 0.97$) and *group*day* ($F(6,252) = 1.20$, $p = 0.30$) or *sex*day* interaction factor ($F(6,252) = 0.22$, $p = 0.96$) s (Table 4).

3.6. Negative geotaxis

Repeated-measures ANOVA for negative geotaxis evaluation did not show differences for *group* ($F(1,28) = 0.02$, $p = 0.87$), but there were significative result for *day* factor, as expected ($F(1,28) = 0.02$, $p = 0.87$) when compared male ZKV to male CT. There were no *group*day* interaction effect ($F(5,140) = 0.44$, $p = 0.81$). When compared female ZKV to female CT there was no *group* effect ($F(1,13) = 2.45$, $p = 0.14$), but there was *day* effect, as expected ($F(5,65) = 132.17$, $p = 0.00$). Additional GLM analysis for repeated measures did not show *group* ($F(1,42) = 0.90$, $p = 0.34$) or *sex* differences ($F(1,42) = 0.12$, $p = 0.73$). No *day* ($F(5,210) = 0.31$, $p = 0.91$), *group*day* ($F(5,210) = 0.31$, $p = 0.90$) or *sex*day* ($F(5,210) = 0.37$, $p = 0.86$) interactions were observed (Table 5).

3.7. Homing behavior

One-way repeated-measures ANOVA for Homing behavior analysis showed a significant difference on *group* when compared male ZKV to male CT ($F(1,28) = 9.25$, $p = 0.005$). Additional *t*-test evidenced higher latency for the ZKV group on PND 12 and PND 15, compared to controls ($t(15) = 2.38$; $P < 0.05$ and $t(15) = 2.39$; $P < 0.05$, respectively). As expected, significant difference was observed on *day* factor ($F(6,128) = 23.88$, $p = 0.00$). There was no *group*day* ($F(6,168) = 1.02$, $p = 0.41$) interaction observed. There was no *group* difference in ANOVA female homing behavior analysis when comparing ZKV to CT groups ($F(1,13) = 2.15$, $p = 0.16$), but *day* factor presents significant result ($F(1,28) = 9.25$, $p = 0.005$). There was no *group*day* interaction effect observed ($F(5,65) = 0.39$, $p = 0.84$). Supplementary repeated measures GLM

Table 3
Analysis of the aversion to fall reflex. Data are expressed as mean ± SEM. (ZKV) animals that had their mothers infected with the *Zika* virus during pregnancy. (CT) Animals of the control group. (PND) postnatal day. Female CT (n = 8); Female ZKV (n = 7); Male CT (n = 15); Male ZKV (n = 15). Repeated-measures ANOVA followed by Tukey's test was performed for each sex comparing ZKV with CT. No differences were found comparing CT and ZKV groups. [a] Indicates significant difference in the CT groups when compared to the first day analyzed. [b] Indicates significant difference in the ZKV groups when compared to the first day analyzed.

Aversion to fall	Female CT	Female ZKV	Male CT	Male ZKV
PND 6	30.00 ± 0.74	29.42 ± 0.80	29.64 ± 0.54	29.15 ± 0.54
PND 9	25.33 ± 1.94	23.47 ± 2.08	23.84 ± 1.42 [a]	25.62 ± 1.42[b]
PND 12	16.95 ± 2.45 [a]	12.80 ± 2.62[b]	14.55 ± 1.79 [a]	14.57 ± 1.79[b]
PND 15	4.87 ± 0.56 [a]	3.76 ± 0.60[b]	4.88 ± 0.41 [a]	4.48 ± 0.41[b]
PND 18	4.29 ± 0.75 [a]	3.19 ± 0.80[b]	4.66 ± 0.55 [a]	3.64 ± 0.55[b]
PND 21	4.25 ± 0.77 [a]	5.57 ± 0.82[b]	3.71 ± 0.56 [a]	3.20 ± 0.56[b]

Table 4
Analysis of the gait. Time to animal leave the circle with a diameter of 30 cm. Data are expressed as mean ± SEM. (ZKV) animals that had their mothers infected with the *Zika* virus during pregnancy. (CT) Animals of the control group. (PND) postnatal day. Female CT (n = 8); Female ZKV (n = 7); Male CT (n = 15); Male ZKV (n = 15). Repeated-measures ANOVA was performed for each sex comparing ZKV with CT. No differences were found comparing CT and ZKV groups. [a] Indicates significant difference to the CT group when compared to the first day analyzed. [b] Indicates significant difference to the ZKV group when compared to the first day analyzed. * Represents difference when compared to CT group of the same sex. One-way ANOVA $p < 0.05$.

Gait	Female CT	Female ZKV	Male CT	Male ZKV
PND 3	27.54 ± 1.00	30.00 ± 1.07	28.64 ± 0.73	29.95 ± 0.73
PND 6	24.50 ± 2.08	27.47 ± 2.22	28.13 ± 1.52	24.44 ± 1.52[b]
PND 9	25.50 ± 29.99	17.61 ± 3.19[b]	21.04 ± 2.18 [a]	20.24 ± 2.18[b]
PND 12	12.16 ± 1.74 [a]	12.04 ± 1.86[b]	14.06 ± 1.27 [a]	11.86 ± 1.27[b]
PND 15	9.33 ± 0.84 [a]	5.00 ± 0.90[b]	6.04 ± 0.61 [a]	7.51 ± 0.61[b]*
PND 18	4.08 ± 0.89 [a]	4.42 ± 0.95[b]	4.64 ± 0.65 [a]	3.53 ± 0.65[b]
PND 21	3.08 ± 0.68 [a]	4.61 ± 0.73[b]	3.71 ± 0.50 [a]	3.13 ± 0.50[b]

Table 5
Analysis of the negative geotaxis reflex. Data are expressed as mean ± SEM. (ZKV) animals that had their mothers infected with the *Zika* virus during pregnancy. (CT) Animals of the control group. (PND) postnatal day. Female CT (n = 8); Female ZKV (n = 7); Male CT (n = 15); Male ZKV (n = 15). Repeated-measures ANOVA followed by Tukey's test was performed for each sex comparing ZKV with CT. No differences were found comparing CT and ZKV groups. No differences were found when compared male ZKV to male CT ($F(1,28) = 0.03$, $p = 0.87$), or when compared female ZKV to female CT ($F(1,13) = 2.45$, $p = 0.14$). [a] Indicates significant difference to the CT groups when compared to the first day analyzed. [b] Indicates significant difference to the ZKV groups when compared to the first day analyzed.

Negative geotaxis	Female CT	Female ZKV	Male CT	Male ZKV
PND 6	30.00 ± 0.74	29.42 ± 0.80	29.64 ± 0.54	29.15 ± 0.54
PND 9	25.33 ± 1.94	23.47 ± 2.08	23.84 ± 1.42 [a]	26.62 ± 1.42
PND 12	16.95 ± 2.45 [a]	12.80 ± 2.62[b]	14.55 ± 1.79 [a]	14.57 ± 1.79[b]
PND 15	4.87 ± 0.56 [a]	3.76 ± 0.60[b]	4.88 ± 0.41 [a]	4.48 ± 0.41[b]
PND 18	4.29 ± 0.75 [a]	3.19 ± 0.80[b]	4.66 ± 0.55 [a]	3.64 ± 0.55[b]
PND 21	4.25 ± 0.77 [a]	5.57 ± 0.82[b]	3.71 ± 0.56 [a]	3.20 ± 0.56[b]

revealed *group* effect (F(1,42) = 12.14, p = 0.01). This effect was specifically observed on PND3 (F(1,42) = 4.35, p = 0.04), PND12 (F(1,42) = 5.14, p = 0.03) and PND21 (F(1,42) = 5.06, p = 0.03) showing higher latency for ZKV group and indicating development delay of these animals. There was no *day* (F(6,252) = 0.87, p = 0.52), *group*day* (F(6,252) = 0.85, p = 0.53 or *sex*day* (F(6,252) = 0.50, p = 0.81) interactions observed (Fig. 2A and 2B).

3.8. Righting reflex

Statistical analysis of the Righting reflex did not evidence differences in group factor when comparing male ZKV to male CT (F(1,28) = 0.79, p = 0.37). However, there was a day effect, evidencing reduced test latency over days (F(2,56) = 14.03, p = 0.00). There were no *group*day* (F(2,56) = 0.78, p = 0.46) interaction effect observed. We found a significant *group* effect when compare female ZKV to female CT (F(1,13) = 8.23, p = 0.01), indicating a delay in development of ZKV animals. This result was confirmed by an additional *t*-test that revealed that the Zika group took more time to perform the Righting reflex on PND 3 (t(13) = 2.11; P = 0.05). There was *day* effect, evidencing reduced test latency over days (F(2,26) = 8.52, p = 0.00), as expected. No interaction *group*day* effect was observed (F(2,26) = 1.49, p = 0.24). Additional repeated measures GLM revealed *group* (F(1,42) = 6.24, p = 0.02) and *sex* (F(1,42) = 6.66, p = 0.01) effects. GLM results showing *group* effects on PND 3 (F(1,42) = 4.12, p = 0.05) and *sex* effect on PND 9 (F(1,42) = 6.19, p = 0.02) confirming delay in righting reflex in ZKV female animals (Fig. 2C and 2D).

3.9. Histological analysis

T-test was performed to compare the number of neurons in the cortex and hippocampus between groups. No statistical difference was found in the hippocampus (t(4) = 1.18; P > 0.05), or cortex (t(6) = 1.01; P > 0.05) in this analysis (Table 6 and Fig. 3).

3.10. Protein immunodetection

To compare the levels of BBB proteins between the ZKV and CT groups on PND 22 the Student T-test was performed. In the hippocampus, T-test revealed a reduction for proteins β-catenin (t(11) = 2.78; P < 0.05), connexin 43 (t(9) = 2.35; P < 0.05), and occludin (t(11) = 2.29; P < 0.05) when compared to CT group. GFAP (t(11) = 0.13; P > 0.05), GLUT-1 (Mann-Whitney test = 21, p > 0,05, n = 6) and aquaporin 4 (Mann-Whitney test = 11, p > 0,05, n = 6) did not present a statistically

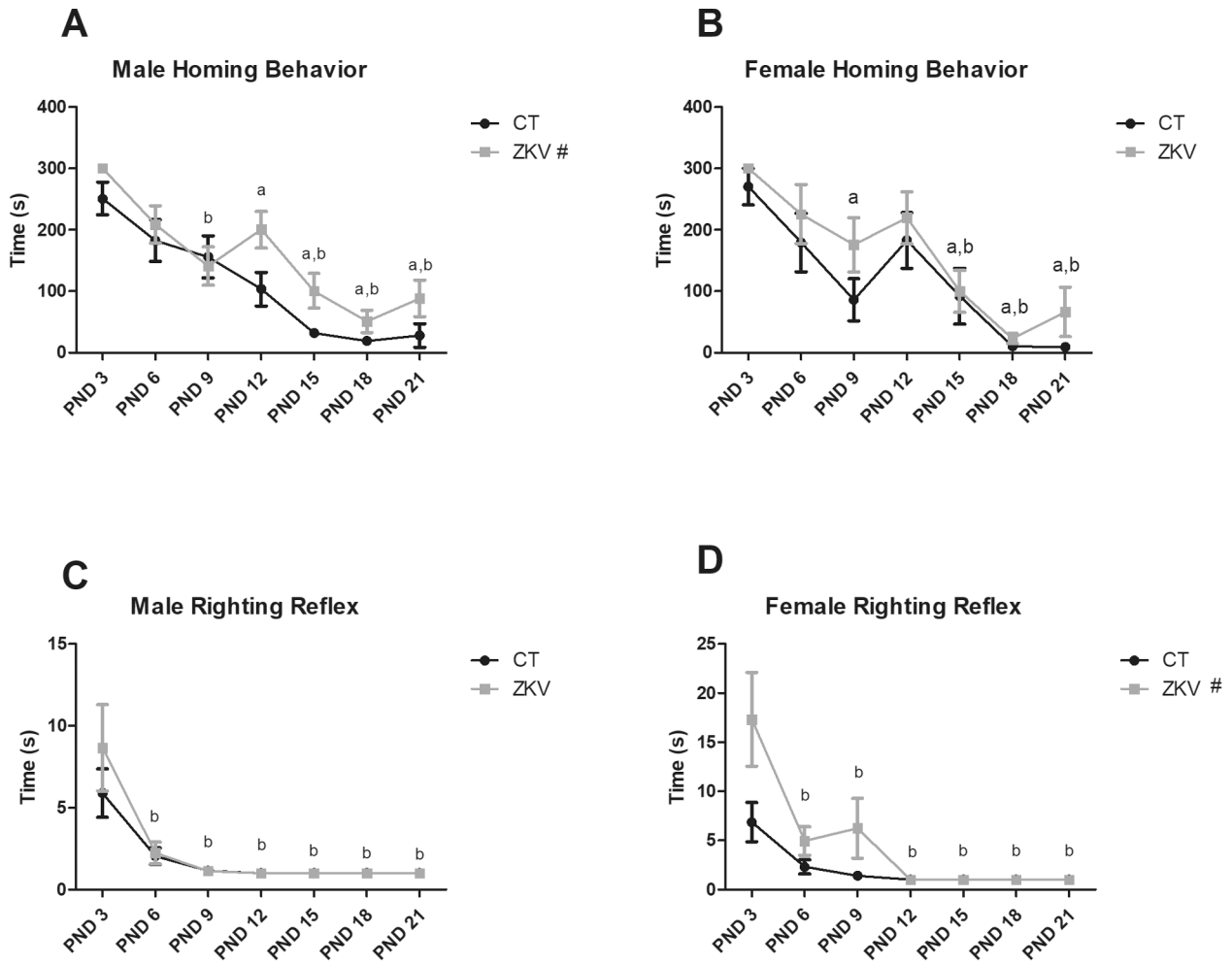

Fig. 2. Analysis of the homing behavior (A) and (B) and righting reflex (C) and (D). Data are expressed as mean ± SEM. (ZKV) animals that had their mothers infected with the *Zika* virus during pregnancy. (CT) Animals of the control group. (PND) postnatal day. Female CT (n = 8); Female ZKV (n = 7); Male CT (n = 15); Male ZKV (n = 15).[(a)] Indicates difference of the CT group when compared to the first day analyzed (PND 3).[(b)] Indicates difference of the ZKV group when compared to the first day analyzed (PND 3). **(A)** # Indicates *group* effect for Male Homing Behavior. Additional *t*-test indicates ZKV male delay on PND 12 and PND 15 (not showed) and GLM repeated measures indicates ZKV delay on PND 3, PND 12 and PND 21 (not showed). **(D)** # Indicates *group* effect for Female Righting Reflex. Additional *t*-test indicates ZKV female delay on PND 3 (not showed) and GLM repeated measures indicates ZKV delay on PND 3, and specifically female delay on PND 9 (not showed). p < 0.05.

Table 6
Neuronal quantification in the hippocampus and cortex. Data are expressed as mean ± SEM. (ZKV) animals that had their mothers infected with the *Zika* virus during pregnancy. (CT) Animals of the control group. Hippocampus CT (n = 3); ZKV (n = 3). Cortex CT (n = 4); ZKV (n = 4). Student T- test for each structure comparing ZKV with CT ($p < 0.05$). No differences were found in this evaluation.

Number of neurons		
Number of neurons		
	ZKV	CT
Hippocampus	50.60 ± 5.77	38.87 ± 2.90
Cortex	44.33 ± 7.79	55 ± 7.01

significant result (Fig. 4). On the other hand, cortical Student T-test did not reveal differences for any of the proteins evaluated: (aquaporin 4 ($t(10) = 1.21$; $P > 0.05$), β-catenin ($t(11) = 0.92$; $P > 0.05$), connexin 43 ($t(11) = 0.05$; $P > 0.05$), GFAP ($t(10) = 1.18$; $P > 0.05$), occludin ($t(9) = 1.09$; $P > 0.05$) and GLUT-1 ($t(10) = 0.85$; $P > 0.05$)) (Fig. 5).

3.11. Redox status evaluation

Student T-test performed on PND 22 in the cortex showed reduction in DCF levels ($t(11) = 3.43$; $P < 0.05$) and SOD activity ($t(11) = 4.11$; $P < 0.05$). CAT activity ($t(11) = 1.37$; $P > 0.05$), Sulfhydryl content ($t(11) = 1.16$; $P > 0.05$) and TBARS ($t(11) = 1.42$; $P > 0.05$) did not presented significant results (Fig. 6). Hippocampal evaluation on PND22 revealed reduction in SOD activity ($t(11) = 2.69$; $P < 0.05$) and Sulfhydryl content ($t(11) = 3.06$; $P < 0.05$). DCF levels ($t(11) = 0.30$; $P > 0.05$), CAT activity ($t(11) = 0.94$; $P > 0.05$) and TBARS ($t(11) = 0.11$; $P > 0.05$) did not reach significative differences (Fig. 7).

4. Discussion

In the current study, we extended the comprehension on congenital ZIKV syndrome by proposing a congenital ZIKV infection rat model aiming to identify neurodevelopmental and brain tissue disturbances in *Wistar* rats, just after birth. The infection was carried out on E9, a critical period for rodents' neurodevelopment (Semple et al., 2013). Pregnant rats were i.p. inoculated and our data revealing virus in the females' blood, six hours after infection; additionally, viable virus in the placenta and spleen of females and in fetuses were also identified, twenty-four hours after inoculation. Interestingly, there were no female's sickness behavior despite puppies' neurological damage, corroborating previous findings (Sherer et al., 2019). This is an important finding since recently

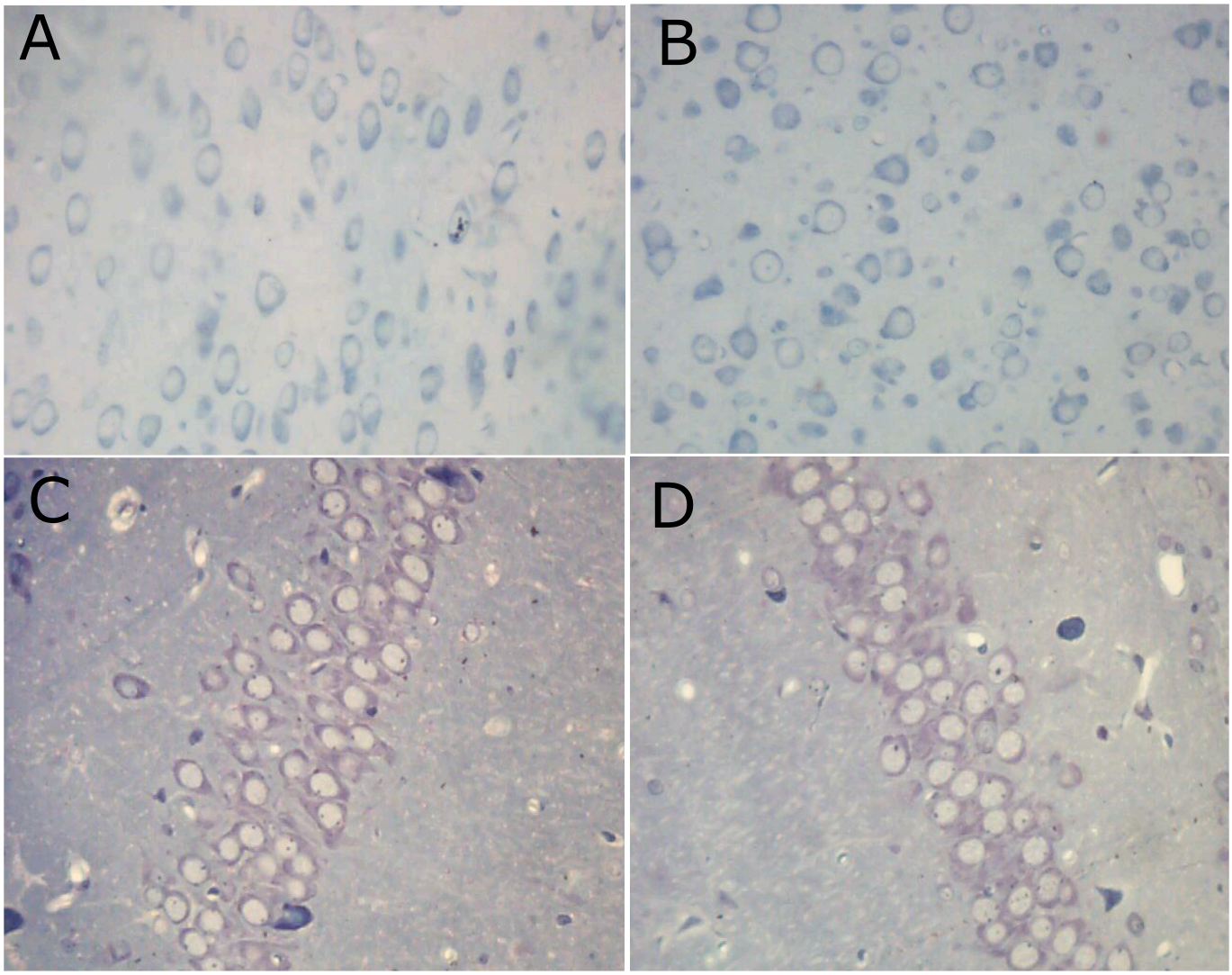

Fig. 3. Representative images of brains sections stained with toluidine blue. (A) Cortical neurons of the CT group. (B) Cortical neurons of the ZKV group. (C) CA1 hippocampal neurons of the CT group. (D) CA1 hippocampal neurons of the ZKV group. 200 X magnification. Hippocampus CT (n = 3); ZKV (n = 3). Cortex CT (n = 4); ZKV (n = 4).

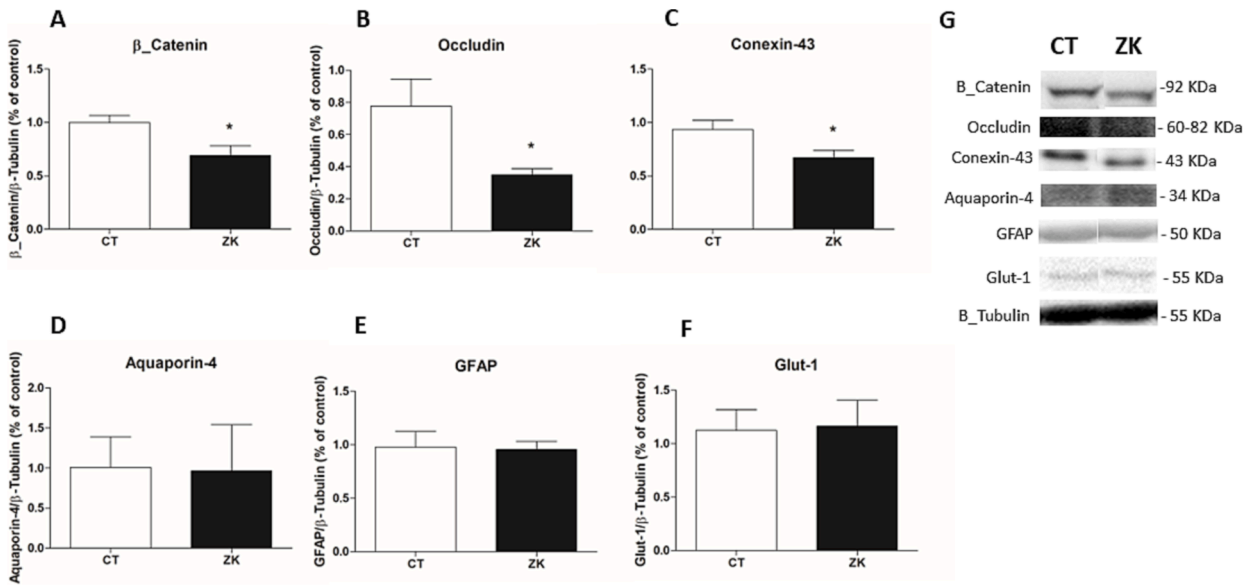

Fig. 4. Quantification of hippocampal blood–brain barrier (BBB) proteins on PND22. (A) β-catenin (B) Occludin (C) Conexin-43 (D) Aquaporin-4 (E) GFAP (F) Glut-1. (G) Representative images of western blotting bands analyzed. Data are expressed as mean ± SEM. (ZKV) animals that had their mothers infected with the *Zika* virus during pregnancy. (CT) Animals of the control group. CT (n = 7) ZKV (n = 6). * Indicates significative result when compared to CT. Student T- test comparing ZKV with CT for each protein, $p < 0.05$. Data is presented as percentage of control.

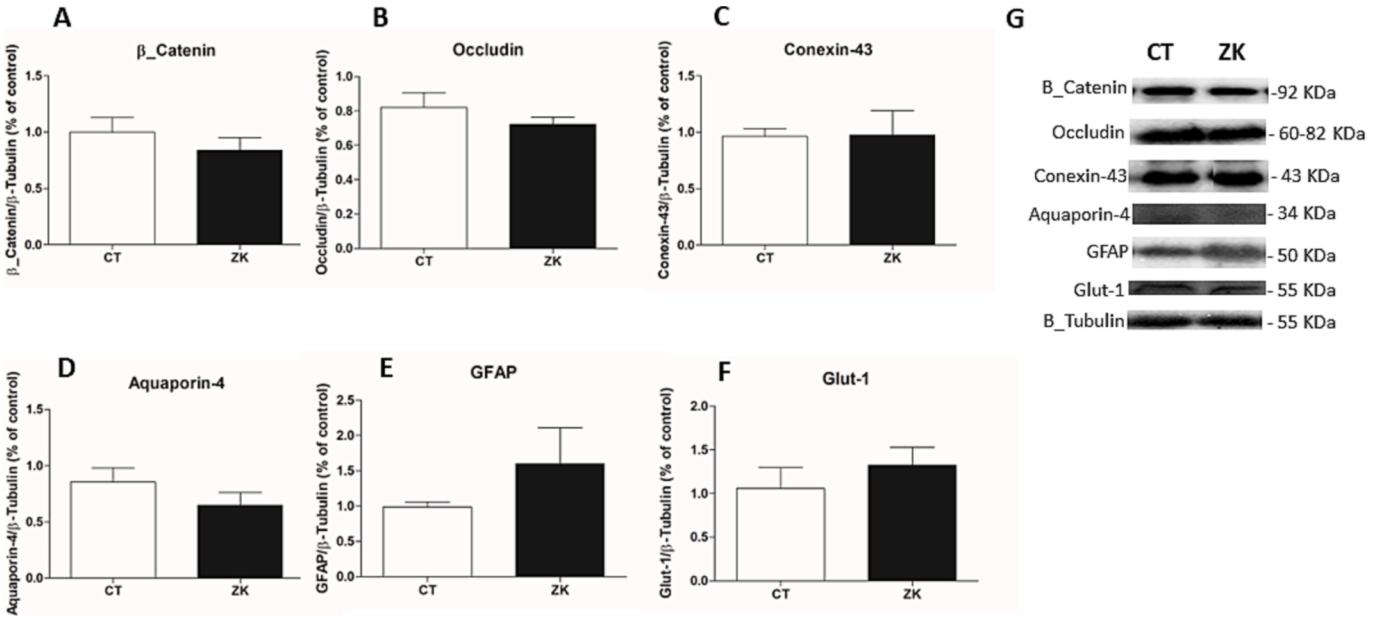

Fig. 5. Quantification of cortical blood–brain barrier (BBB) proteins on PND22. (A) β-catenin (B) Occludin (C) Conexin-43 (D) Aquaporin-4 (E) GFAP (F) Glut-1. (G) Representative images of western blotting bands analyzed. Data are expressed as mean ± SEM. (ZKV) animals that had their mothers infected with the *Zika* virus during pregnancy. (CT) Animals of the control group. CT (n = 7) ZKV (n = 6). Student T- test comparing ZKV with CT for each protein, $p < 0.05$. Data is presented as percentage of control. No differences were found.

it has already been identified ZIKV circulation in asymptomatic pregnant women in Brazilian Northeast region (Branco et al., 2021). Moreover, there is evidence that even in asymptomatic pregnant, the offspring neurodevelopment can be compromised (Shapiro-Mendoza et al., 2017). In consonance, our study revealed important deficiencies in pups' neurobehavioral assessments, which could be considered predictive of both cognitive and/or motor disturbances throughout the life. In addition, on PND 22, BBB integrity deficits in the hippocampus and oxidative status alteration in the hippocampus and cortex were found, which strongly indicate that the virus may exert profound long-term implications on brain structure and function.

In American territories, ZIKV epidemic was marked by the direct correlation between the gestational ZIKV infection and the expressive increased of microcephaly incidence, an important congenital malformation observed in children soon after birth, mainly identified in the northeast of Brazil (Calvet et al., 2016; Martines et al., 2016). Thus, in our experimental study, rats body measurements were performed, including head measurements, to verify whether this finding also could occur in the proposed animal model. We did not find changes on rats body measurements nor on head size. Although, previous studies have already drawn attention to the neurodevelopmental outcomes that could be identified even without microcephaly (Aragao et al., 2017; Cardoso

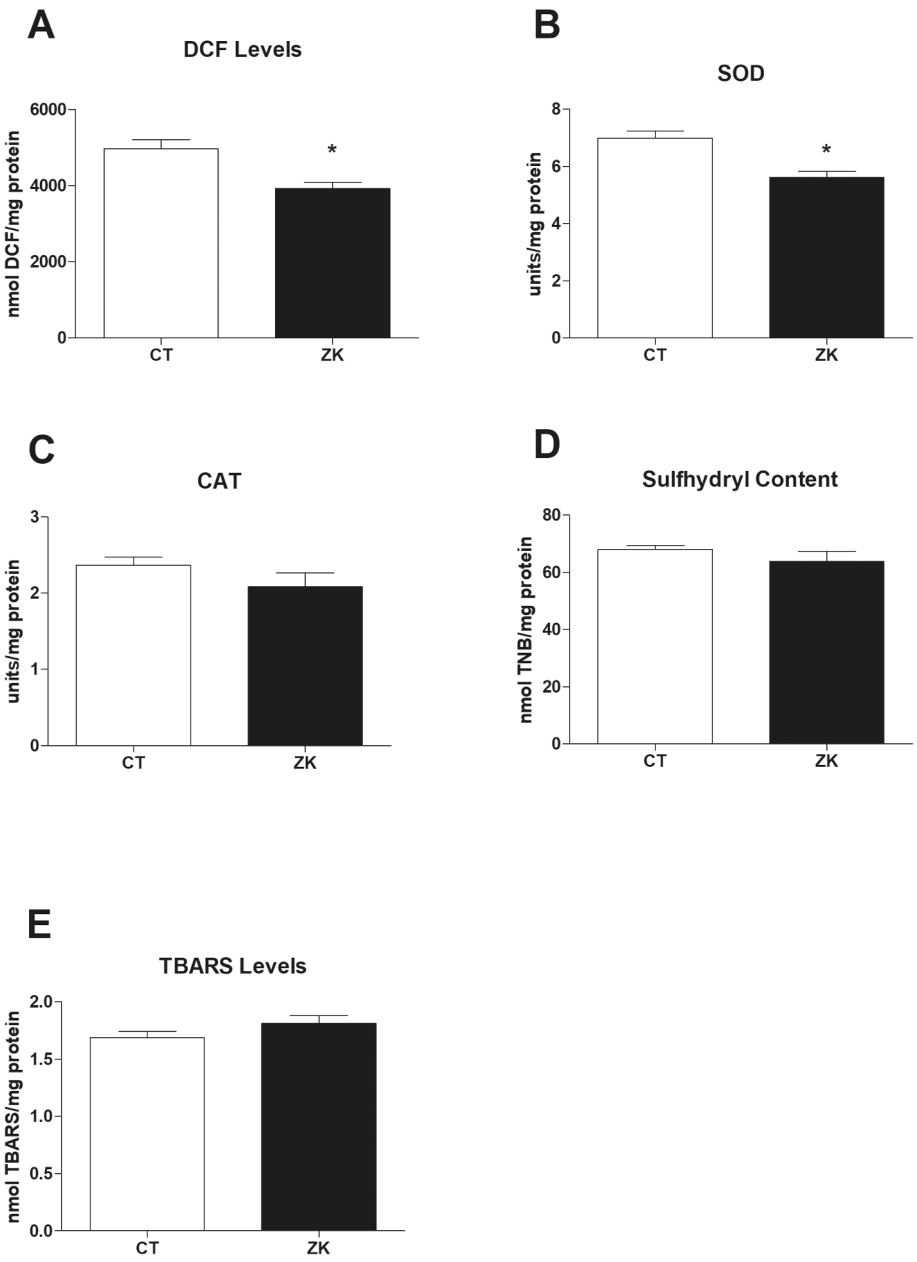

Fig. 6. Cortical redox status evaluation on PND22. (A) DCF (2′,7′-Dichlorofluorescein) levels (B) Superoxide dismutase (SOD) activity (C) Catalase (CAT) activity (D) Sulfhydryl content (E) Thiobarbituric acid-reactive substances (TBARS) levels. (ZKV) animals that had their mothers infected with Zika virus during pregnancy. (CT) Animals of the control group. CT (n = 7) ZKV (n = 6). * Indicates significative result when compared to CT. Results are expressed as mean ± SEM Student T- test, $p < 0.05$.

et al., 2019). In this way, the present study has investigated neurobehavioral development to identify offspring sequel consequent to congenital ZIKV infection.

Neurodevelopmental assessments allow early identification of children's development delay, being essential for primary health care, primarily in the early child's life. Thus, it is possible to quickly start intervention services and provide means for early childhood education services and families to act, as soon as possible, preventing the worsening of the condition and granting the brief start of therapeutic actions (Liu et al., 2010; Sandler et al., 2001). From translational perspective rodents' neurodevelopmental assessments (or developmental milestones) make possible inferring on the sensorimotor and cognitive animals' development (Smirnov & Sitnikova, 2019), being an indicative for developmental disorders in adulthood (Nguyen et al., 2017). In our study, we found some developmental milestones delay in the ZIKV group; incisor tooth eruption, forelimb placing (unilateral), hind limb placing (bilateral), and forelimb grasp (unilateral) were identified later in male ZIKV rats and hind limb placing (bilateral) and righting reflex in female rats, compared to controls, showing that both sex are affected. This is a remarkable result, since even in severe nervous system injuries, as caused by experimental neonatal hypoxia–ischemia (HI), no neurodevelopmental assessment impairments were detected (Deniz et al., 2018; Schuch et al., 2016). We additionally identified righting reflex delay in females, besides gait and homing behavior dysfunction in males, once again revealing both sex retarded performance. Righting reflex disruption has also been identified in HI animal model (Lubics et al., 2005; Sanches et al., 2012a; Sanches et al., 2012b) as well homing behavior deficits (Sanches et al., 2012a; Sanches et al., 2012b). In consonance with our findings, a study that used immunocompetent mice also did not find alterations in the phenotype at birth after the ZIKV infection, but later learning and memory impairments were observed (Stanelle-Bertram et al., 2018). Also, a recent clinical study performed with mothers who had ZIKV infection during pregnancy observed children asymptomatic at birth but showing the emergence of at least one developmental delay marker (Maia et al., 2021). In consonance, we observed that our congenital animal model was able to reproduce

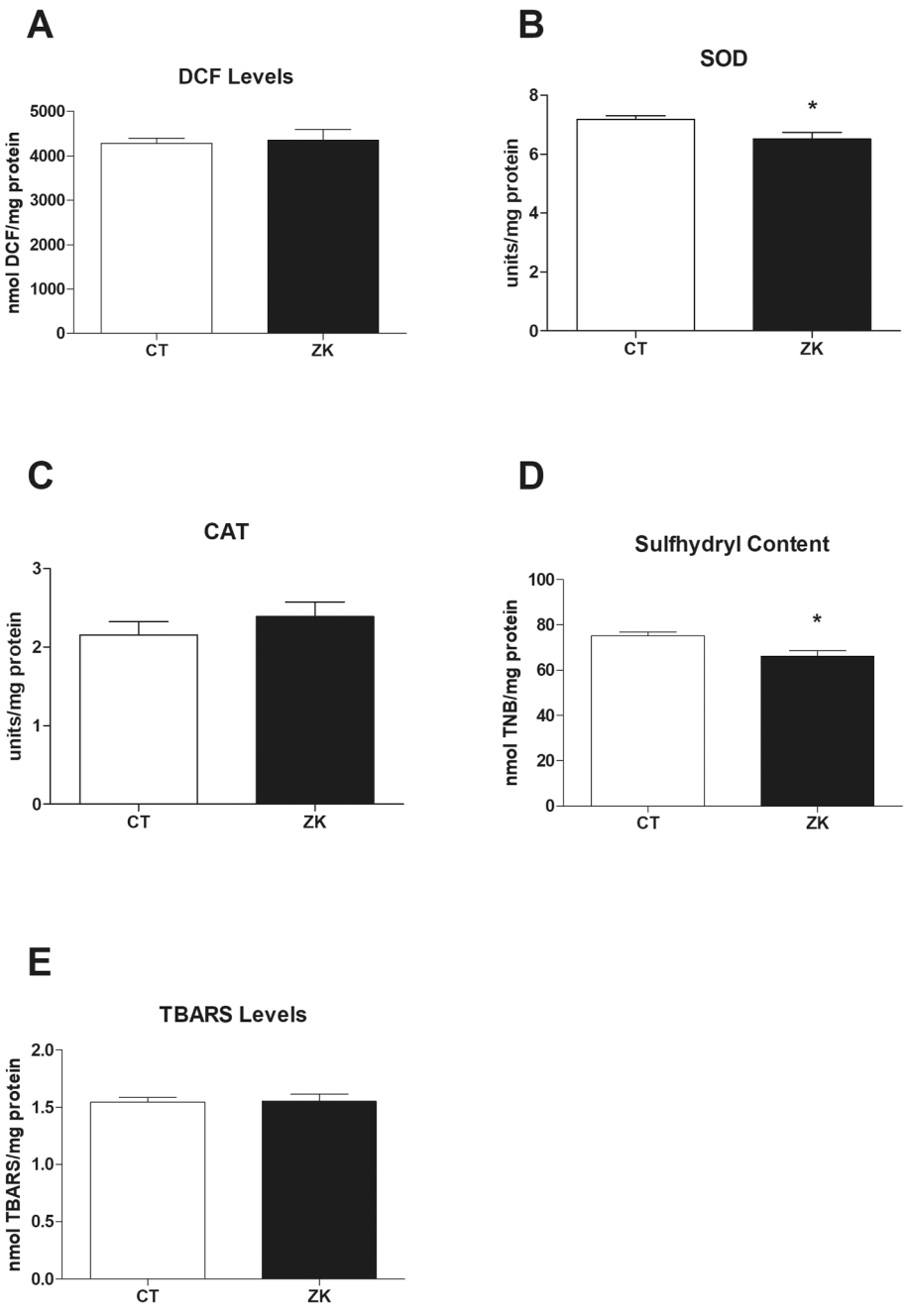

Fig. 7. Hippocampal redox status evaluation on PND22. (A) DCF (2′,7′-Dichlorofluorescein) levels (B) Superoxide dismutase (SOD) activity (C) Catalase (CAT) activity (D) Sulfhydryl content (E) Thiobarbituric acid-reactive substances (TBARS) levels. (ZKV) animals that had their mothers infected with Zika virus during pregnancy. (CT) Animals of the control group. CT (n = 7) ZKV (n = 6). * Indicates significative result when compared to CT. Results are expressed as mean ± SEM Student T- test, $p < 0.05$.

developmental delay, as observed in children. Following the timeline of pathological investigation, seeking to advance with the damage understood from the proposed model, we evaluated tissue integrity assessing neuronal number, BBB integrity and redox status of the hippocampus and cortex on PND22.

Studies with viral mice inoculation, carried out directly in the neonate just after birth, have identified neuronal death and overall brain damage (cortex, hippocampus, and spinal cord) (S. Li et al., 2018; Y. Li et al., 2021). Cortical layer thickness reduction was also observed when congenital infection was performed in pregnant mice, revealing cell death and consequent tissue atrophy (Cugola et al., 2016). Nonetheless, no difference on the cortex or hippocampus neuronal count was found. This data can justify the absence of head reduction observed in the current work, since there was no expressive tissue loss. So, we seek to improve the assessment of tissue integrity, evaluating the BBB structure focusing on its main constituent proteins.

BBB is an interface that evolves brain and spinal cord and is composed by the endothelial cells, pericyte, astrocyte endfeet and basal membrane (Geng et al., 2018). The maintenance of BBB integrity is fundamental for the nervous tissue homeostasis, so permeability disturbances resulting from failures in the tight junctions/adhesive junction proteins are key factors to be considered (Obermeier et al., 2013). Furthermore, BBB disruption is strongly associated to cognitive impairments (Barisano et al., 2022; Geng et al., 2018) and neurodevelopmental damages (Diaz et al., 2016). In our study, we identified on hippocampus an important reduction in β-catenin, Occludin and Conexin-43 proteins, essential BBB components. Previous work with *in vitro* modeling BBB subjected to Zika infection showed that virus infected endothelial cells, and crossed the barrier, however in this study there was no evidence of BBB disruption (Alimonti et al., 2018). On the other hand, an *in vitro* human BBB model based on brain-like endothelial cells (hBLECs), occludin, claudin 5, and ZO-1 was downregulated by

ZIKV, and partial perturbation of BBB permeability was detected (Clé et al., 2020). Yet, another study showed that ZIKV alters *in vitro* expression of tight junction, downregulating claudin-5 and occludin and upregulating ZO-1 were identified. In the same study, *in vivo* infection also caused reduction in claudin-5 expression evaluated on 2 dpi and affected BBB integrity (Leda et al., 2019). Interestingly, a study with brain cell preparations showed that ZIKV infection promotes an upregulation of inflammatory mediators such as interleukin 6 (IL-6), tumor necrosis factor alpha (TNF-α) and interleukin 1β (IL-1β) (Lum et al., 2017); expression of inflammatory factors has also been identified in hBLECs human BBB model and may trigger the recruitment of immune cells and promote additional local inflammation (Clé et al., 2020). The relationship between BBB dysfunction and neuroinflammation, as a pathological mark in ZKV infection, was recently cited (Panganiban et al., 2020). These authors observed fibrinogen extravasation (adopted as a measure of BBB disturbance) associated to increased inflammatory hallmarks in the nervous system using a ZIKV primate model. The present study advanced towards a more specific comprehension on BBB, revealing that this important protection to brain parenchyma was widely and structurally affected consequent to ZIKV infection. It is worth to mention that the infection in our model was carried out in E9 and BBB constituents' alterations were identified on DPN22, revealing that such changes appear to be persistent, thereby contributing to long-term effects of the prenatal ZIKV infection.

Beyond the implication on the neuroinflammation, it has already been demonstrated that BBB disruption may also be correlated with oxidative stress and both changes have already been identified after ZIKV infection, emerging as important neuropathological features (Almeida et al., 2020; Clé et al., 2020; Obermeier et al., 2013; Panganiban et al., 2020). In this line, we sought to identify whether oxidative stress could also be identified in our rat model. A homeostatic imbalance in reactive oxygen species (ROS) production or the suppression of intracellular antioxidant defenses can lead to oxidative stress, causing widespread intracellular damage and even cell death (Burton & Jauniaux, 2011). In addition, ROS increase is intrinsically related to BBB damage through oxidative injury and constitutive BBB proteins modulation (Obermeier et al., 2013; Pun et al., 2009). Present data concerning redox state demonstrated hippocampal and cortical SOD activity reduction, hippocampal Sulfhydryl content and cortical DCF levels reduction, that clearly have indicated a ROS imbalance. ROS changes and astrocytic reactivity was previously observed *in vitro* by observing iPSC-derived astrocytes and C57BL/6 mice infected with ZIKV (Ledur et al., 2020); also, SOD and CAT activity decrease have already been reported after ZIKV infection *in vitro* (using U87-MG and HepG2 cell lines) and *in vivo* (using C57BL/6 mice), with the infection carried out directly in the pups (Almeida et al., 2020). It is noteworthy to highlight that this imbalance, on BBB function and oxidative status, is identified in offspring brain tissue, confirming that ZIKV gestational infection resulted in a congenital syndrome in rats, even with their immune system functionally intact. To our knowledge, this is the first evidence of a long-term oxidative stress after congenital ZIKV infection, as observed in our study. Altogether, even without reduction in head circumference and without major morphological changes or neuronal counting, we found brain ROS imbalance in addition to decreased protein immunocontent of main BBB constituents on PND 22. Therefore, it is reasonable to consider that this result set can be directly responsible for the critical delay in the neurodevelopmental assessments observed.

5. Conclusion

Our study sought to extend the understanding of the impairment caused after gestational ZIKV infection, proposing a model with immunocompetent rats, and seeking to identify neurobehavioral assessments predictive of long-term disabilities. In conclusion, we have identified that even without brain morphometric alterations and microcephaly-like phenotype, it was found to have important developmental deficits associated to hippocampal and cortical BBB damage and ROS imbalance, twenty-two days after birth. Such data taken together evidenced that the impairment resulting from gestational infection could be extended for a long time. Our study added to current knowledge of the literature, highlighting the importance of improving prenatal diagnosis, early intervention and long-term studies that advance the understanding of the mechanisms behind the congenital ZIKV syndrome. The development of a more reliable congenital model of ZIKV infection provides additional evidence for understanding the congenital pathology as well as give opportunities for the development of new and improved treatment strategies.

Declaration of Competing Interest

The authors declare that they have no known competing financial interests or personal relationships that could have appeared to influence the work reported in this paper.

Data availability

Data will be made available on request.

Acknowledgments

The authors are extremely thankful to professor Dr. Matilde Achaval, PhD, and would like to pay a posthumous tribute to founder of the Laboratório de Histofisiologia Comparada and co-founder of the Postgraduate Program in Neurosciences at UFRGS. For decades, Dr. Achaval contributed to the structure improvement of the Postgraduate Program in Neurosciences at UFRGS and influenced numerous neuroscientists. Her memorable example of dedication inspired us to follow her scientific path and left those who knew her work eternally grateful.

The authors would like to thank Maikel Oliveira and Chris Krebs for technical support and Centro de Reprodução e Experimentação de Animais de Laboratório (CREAL/ICBS/UFRSG) for the structure and staff support to NB-2 procedures.

Funding Statement

This study was supported by the Brazilian funding agencies: FAPERGS (51/2551-0001975-1), CNPq (428198/2018-0 universal), and CAPES. de Almeida W, dos Santos A. S, were supported by a scholarship from CAPES. Pereira L. O., Wyse A. T. S., and Roehe P. M. are CNPq investigators.

Ethics Approval Statement

Experimental procedures were approved by the Research Ethics Committee of the Universidade Federal do Rio Grande do Sul - *UFRGS, Brazil* (n°. 33452).

Author contributions

Almeida. W and Pereira L. O developed the study concept and protocol design. dos Santos A. S., and Faustino A. M, contributed to the development of the animal protocols. Deniz B. F., and Faustino A. M have assisted in morphological and behavioral studies. Wyse A. T. S., Schmitz F., and Junior O. V. R., contributed with oxidative stress assay. Varela A. P. M., Teixeira T. F., and Roehe P. M contributed with viral procedures, RNA extraction and qPCR analysis. Sesterheim P., and Silva F. M contributed to procedures and analysis of ZIKV detection and quantification in the placenta and fetuses. Almeida, W matched the experimental procedures, analyzed data, and wrote the manuscript. Pereira L. O supervised the study.

Data Availability Statement

Data available on reasonable request from the authors.

Appendix A. Supplementary data

Supplementary data to this article can be found online at https://doi.

org/10.1016/j.bbi.2023.04.014.

References

Alimonti, J.B., Ribecco-Lutkiewicz, M., Sodja, C., Jezierski, A., Stanimirovic, D.B., Liu, Q., Haqqani, A.S., Conlan, W., Bani-Yaghoub, M., 2018. Zika virus crosses an in vitro human blood brain barrier model. Fluid. Barrier. CNS 15 (1). https://doi.org/10.1186/S12987-018-0100-Y.

Almeida, L.T., Ferraz, A.C., da Silva Caetano, C.C., da Silva Menegatto, M.B., dos Santos Pereira Andrade, A.C., Lima, R.L.S., Camini, F.C., Pereira, S.H., da Silva Pereira, K.Y., de Mello Silva, B., Perucci, L.O., Talvani, A., de Magalhães, J.C., de Brito Magalhães, C.L., 2020. Zika virus induces oxidative stress and decreases antioxidant enzyme activities in vitro and in vivo. Virus Res. 286, 198084.

Alvarado, M.G., Schwartz, D.A., 2017. Zika Virus Infection in Pregnancy, Microcephaly, and Maternal and Fetal Health: What We Think, What We Know, and What We Think We Know. Arch. Pathol. Lab. Med. 141 (1), 26–32. https://doi.org/10.5858/arpa.2016-0382-RA.

Aragao, M.F.V.V., Holanda, A.C., Brainer-Lima, A.M., Petribu, N.C.L., Castillo, M., van der Linden, V., Serpa, S.C., Tenório, A.G., Travassos, P.T.C., Cordeiro, M.T., Sarteschi, C., Valenca, M.M., Costello, A., 2017. Nonmicrocephalic Infants with Congenital Zika Syndrome Suspected Only after Neuroimaging Evaluation Compared with Those with Microcephaly at Birth and Postnatally: How Large Is the Zika Virus "Iceberg"? *AJNR Am J Neuroradiol.* 38 (7), 1427–1434.

Barisano, G., Montagne, A., Kisler, K., Schneider, J. A., Wardlaw, J. M., & Zlokovic, B. v. (2022). Blood–brain barrier link to human cognitive impairment and Alzheimer's disease. *Nature Cardiovascul. Res. 2022 1:2*, *1*(2), 108–115. https://doi.org/10.1038/s44161-021-00014-4.

Branco, R. C. C., Brasil, P., Araújo, J. M. G., Cardoso, F. O., Batista, Z. S., Leitão, V. M. S., da Silva, M. A. C. N., de Castro, L. O., Valverde, J. G., Jeronimo, S. M. B., Lima, J. A., Ribeiro da Silva, R., Barbosa, M. D. C. L., Brito, L. M. O., Xavier, M. A. P., & Nascimento, M. D. D. S. B. (2021). Evidence of Zika virus circulation in asymptomatic pregnant women in Northeast, Brazil. *PLoS neglected tropical diseases*, *15*(6), e0009412. https://doi.org/10.1371/journal.pntd.0009412.

Burton, G.J., Jauniaux, E., 2011. Oxidative stress. Best Pract. Res. Clin. Obstet. Gynaecol. 25 (3), 287. https://doi.org/10.1016/J.BPOBGYN.2010.10.016.

Calvet, G., Aguiar, R. S., Melo, A. S., Sampaio, S. A., de Filippis, I., Fabri, A., Araujo, E. S., de Sequeira, P. C., de Mendonca, M. C., de Oliveira, L., Tschoeke, D. A., Schrago, C. G., Thompson, F. L., Brasil, P., dos Santos, F. B., Nogueira, R. M., Tanuri, A., & de Filippis, A. M. (2016). Detection and sequencing of Zika virus from amniotic fluid of fetuses with microcephaly in Brazil: a case study. *Lancet Infect Dis*, *16*(6), 653–660. https://doi.org/S1473-3099(16)00095-5 [pii] 10.1016/S1473-3099(16)00095-5.

Cardoso, T.F., dos Santos, R.S., Corrêa, R.M., Campos, J.V., Silva, R.D.B., Tobias, C.C., Prata-Barbosa, A., da Cunha, A.J.L.A., Ferreira, H.C., 2019. Congenital Zika infection: neurology can occur without microcephaly. Arch. Dis. Child. 104 (2), 199–200. https://doi.org/10.1136/ARCHDISCHILD-2018-314782.

Clé, M., Desmetz, C., Barthelemy, J., Martin, M.-F., Constant, O., Maarifi, G., Foulongne, V., Bolloré, K., Glasson, Y., De Bock, F., Blaquiere, M., Dehouck, L., Pirot, N., Tuaillon, E., Nisole, S., Najioullah, F., Van de Perre, P., Cabié, A., Marchi, N., Gosselet, F., Simonin, Y., Salinas, S., Diamond, M.S., 2020. Zika Virus Infection Promotes Local Inflammation, Cell Adhesion Molecule Upregulation, and Leukocyte Recruitment at the Blood-Brain Barrier. MBio 11 (4). https://doi.org/10.1128/MBIO.01183-20.

Coyne, C. B., & Lazear, H. M. (2016). Zika virus - reigniting the TORCH. *Nat Rev Microbiol*, *14*(11), 707–715. https://doi.org/nrmicro.2016.125 [pii] 10.1038/nrmicro.2016.125.

Cugola, F.R., Fernandes, I.R., Russo, F.B., Freitas, B.C., Dias, J.L.M., Guimarães, K.P., Benazzato, C., Almeida, N., Pignatari, G.C., Romero, S., Polonio, C.M., Cunha, I., Freitas, C.L., Brandão, W.N., Rossato, C., Andrade, D.G., Faria, D.d.P., Garcez, A.T., Buchpigel, C.A., Braconi, C.T., Mendes, E., Sall, A.A., Zanotto, P.M.d.A., Peron, J.P. S., Muotri, A.R., Beltrão-Braga, P.C.B., 2016. The Brazilian Zika virus strain causes birth defects in experimental models. Nature 534 (7606), 267–271.

Dangsagul W, Ruchusatsawat K, Tawatsin A, Changsom D, Noisumdaeng P, Putchakarn S, Phatihattakorn C, Auewarakul P, Puthavathana P. Zika virus isolation, propagation, and quantification using multiple methods. PLoS One. 2021 Jul 30;16(7):e0255314. doi: 10.1371/journal.pone.0255314. PMID: 34329309; PMCID: PMC8323943.

Deniz, B.F., Confortim, H.D., Deckmann, I., Miguel, P.M., Bronauth, L., Oliveira, B.C., Vieira, M.C., Santos, T.M., Bertó, C.G., Hartwig, J., Wyse, Â.T., de, S., Pereira, L.O., 2018. Gestational folic acid supplementation does not affects the maternal behavior and the early development of rats submitted to neonatal hypoxia-ischemia but the high supplementation impairs the dam's memory and the Na +, K + - ATPase activity in the pup's. Int. J. Dev. Neurosci. 71 (1), 181–192. https://doi.org/10.1016/j.ijdevneu.2018.10.001.

Diaz, R., Miguel, P.M., Deniz, B.F., Confortim, H.D., Barbosa, S., Mendonça, M.C.P., da Cruz-Höfling, M.A., Pereira, L.O., Mendonca, M.C.P., da Cruz-Hofling, M.A., Pereira, L.O., 2016. Environmental enrichment attenuates the blood brain barrier dysfunction induced by the neonatal hypoxia-ischemia. Int. J. Dev. Neurosci. 53, 35–45. https://doi.org/10.1016/j.ijdevneu.2016.06.006. https://S0736-5748(16)30055-7 [pii].

El-Dib, M., Massaro, A.N., Glass, P., Aly, H., 2012. Neurobehavioral assessment as a predictor of neurodevelopmental outcome in preterm infants. J Perinatol. Off. J. California Perinatal Associat. 32 (4), 299–303. https://doi.org/10.1038/JP.2011.100.

Geng, J., Wang, L., Zhang, L., Qin, C., Song, Y., Ma, Y., Chen, Y., Chen, S., Wang, Y., Zhang, Z., Yang, G.Y., 2018. Blood-brain barrier disruption induced cognitive impairment is associated with increase of inflammatory cytokine. Front. Aging Neurosci. 10 (MAY), 129. https://doi.org/10.3389/FNAGI.2018.00129/BIBTEX.

Guide for the Care and Use of Laboratory Animals. (2011). In *Guide for the Care and Use of Laboratory Animals*. National Academies Press. https://doi.org/10.17226/12910.

Jacobson, C.F., Stump, D.G., Nemec, M.D., Holson, J.F., DeSesso, J.M., Jacobson, F., Stump, D.G., Mark, C., 1999. Appropriate Exposure Routes and Doses in Studies Designed to Assess Developmental Toxicity: A Case Study of Inorganic Arsenic. Int. J. Toxicol. 18 (5), 361–368. https://doi.org/10.1080/109158199225279.

Kielkopf, C.L., Bauer, W., Urbatsch, I.L., 2020. Bradford Assay for Determining Protein Concentration. Cold Spring Harb Protoc 2020 (4), 136–138. https://doi.org/10.1101/PDB.PROT102269.

Kim, K. C., Kim, P., Go, H. S., Choi, C. S., Yang, S. I., Cheong, J. H., Shin, C. Y., & Ko, K. H. (2011). The critical period of valproate exposure to induce autistic symptoms in Sprague-Dawley rats. *Toxicol Lett*, *201*(2), 137–142. https://doi.org/S0378-4274(10)01813-8 [pii] 10.1016/j.toxlet.2010.12.018.

Kublin, J.L., Whitney, J.B., 2018. Zika Virus Research Models. Virus Res. 254, 15. https://doi.org/10.1016/J.VIRUSRES.2017.07.025.

Lanciotti, R.S., Kosoy, O.L., Laven, J.J., Velez, J.O., Lambert, A.J., Johnson, A.J., Stanfield, S.M., Duffy, M.R., 2008. Genetic and Serologic Properties of Zika Virus Associated with an Epidemic, Yap State, Micronesia, 2007. Emerg. Infect. Dis. 14 (8), 1232. https://doi.org/10.3201/EID1408.080287.

Lazear, H.M., Govero, J., Smith, A.M., Platt, D.J., Fernandez, E., Miner, J.J., Diamond, M. S., 2016. A Mouse Model of Zika Virus Pathogenesis. Cell Host Microbe 19 (5), 720–730. https://doi.org/10.1016/J.CHOM.2016.03.010.

Leda, A.R., Bertrand, L., Andras, I.E., El-Hage, N., Nair, M., Toborek, M., 2019. Selective Disruption of the Blood-Brain Barrier by Zika Virus. Front. Microbiol. 10 https://doi.org/10.3389/FMICB.2019.02158.

Ledur, P.F., Karmirian, K., Pedrosa, C.d.S.G., et al., 2020. Zika virus infection leads to mitochondrial failure, oxidative stress and DNA damage in human iPSC-derived astrocytes. Sci. Rep. 10, 1218. https://doi.org/10.1038/s41598-020-57914-x.

Li, S., Armstrong, N., Zhao, H., Hou, W., Liu, J., Chen, C., Wan, J., Wang, W., Zhong, C., Liu, C., Zhu, H., Xia, N., Cheng, T., Tang, Q., 2018. Zika Virus Fatally Infects Wild Type Neonatal Mice and Replicates in Central Nervous System. Viruses 10 (1). https://doi.org/10.3390/V10010049.

Li, Y., Shi, S., Xia, F., Shan, C., Ha, Y., Zou, J., Adam, A., Zhang, M., Wang, T., Liu, H., Shi, P.Y., Zhang, W., 2021. Zika virus induces neuronal and vascular degeneration in developing mouse retina. Acta Neuropathol. Commun. 9 (1) https://doi.org/10.1186/S40478-021-01195-6.

Li, C., Xu, D., Ye, Q., Hong, S., Jiang, Y., Liu, X., Zhang, N., Shi, L., Qin, C.-F., Xu, Z., 2016. Zika Virus Disrupts Neural Progenitor Development and Leads to Microcephaly in Mice. Cell Stem Cell 19 (1), 120–126.

Liu, J., Bann, C., Lester, B., Tronick, E., Das, A., Lagasse, L., Bauer, C., Shankaran, S., Bada, H., 2010. Neonatal Neurobehavior Predicts Medical and Behavioral Outcome. Pediatrics 125 (1), e90.

Lubics, A., Reglodi, D., Tamas, A., Kiss, P., Szalai, M., Szalontay, L., Lengvari, I., Szalontay, L., & Lengvári, I. (2005). Neurological reflexes and early motor behavior in rats subjected to neonatal hypoxic-ischemic injury. *Behav Brain Res*, *157*(1), 157–165. https://doi.org/S0166-4328(04)00253-0 [pii] 10.1016/j.bbr.2004.06.019.

Lum, F.M., Low, D.K.S., Fan, Y., Tan, J.J.L., Lee, B., Chan, J.K.Y., Rénia, L., Ginhoux, F., Ng, L.F.P., 2017. Zika Virus Infects Human Fetal Brain Microglia and Induces Inflammation. Clin. Infect. Dis. 64 (7), 914–920. https://doi.org/10.1093/CID/CIW878.

Maia, A.M.P.C., Azevedo, C.D.S.L., de Oliveira, R.D.M.A.B., Barreto, F.K.A., Rodrigues, A. S.R., Simião, A.R., Gomes, I.P., Ribeiro, E.M., Cavalcanti, L.P.D.G., 2021. Neurological growth and development of children asymptomatic at birth whose mothers had Zika during pregnancy. Rev. Soc. Bras. Med. Trop. 54, 1–8. https://doi.org/10.1590/0037-8682-0180-2020.

Martines, R.B., Bhatnagar, J., Keating, M.K., Silva-Flannery, L., Muehlenbachs, A., Gary, J., Goldsmith, C., Hale, G., Ritter, J., Rollin, D., Shieh, W.-J., Luz, K.G., Ramos, A.M.d.O., Davi, H.P.F., Kleber de Oliveria, W., Lanciotti, R., Lambert, A., Zaki, S., 2016. Notes from the Field: Evidence of Zika Virus Infection in Brain and Placental Tissues from Two Congenitally Infected Newborns and Two Fetal Losses-Brazil, 2015. MMWR Morb. Mortal. Wkly Rep. 65 (06), 159–160.

Miner, J.J., Sene, A., Richner, J.M., Smith, A.M., Santeford, A., Ban, N., Weger-Lucarelli, J., Manzella, F., Rückert, C., Govero, J., Noguchi, K.K., Ebel, G.D., Diamond, M.S., Apte, R.S., 2016. Zika Virus Infection in Mice Causes Panuveitis with Shedding of Virus in Tears. Cell Rep. 16 (12), 3208–3218. https://doi.org/10.1016/J.CELREP.2016.08.079.

Morrison, T.E., Diamond, M.S., Pierson, T.C., 2017. Animal Models of Zika Virus Infection, Pathogenesis, and Immunity. J. Virol. 91 (8) https://doi.org/10.1128/JVI.00009-17.

Nguyen, A.T., Armstrong, E.A., Yager, J.Y., 2017. Neurodevelopmental Reflex Testing in Neonatal Rat Pups. J. Visual. Exp. : JoVE 2017 (122). https://doi.org/10.3791/55261.

Obermeier, B., Daneman, R., Ransohoff, R.M., 2013. Development, maintenance and disruption of the blood-brain barrier. Nat. Med. 19 (12), 1584–1596. https://doi.org/10.1038/NM.3407.

Oliveira, D., Durigon, G., Mendes, É., Ladner, J., Andreata-Santos, R., Araujo, D., Botosso, V., Paola, N., Neto, D., Cunha, M., Braconi, C., Alves, R., Jesus, M., Pereira, L., Melo, S., Mesquita, F., Silveira, V., Thomazelli, L., Favoretto, S., Almonfrey, F., Abdulkader, R., Gabrili, J., Tambourgi, D., Oliveira, S., Prieto, K., Wiley, M., Ferreira, L., Silva, M., Palacios, G., Zanotto, P., Durigon, E., 2018. Persistence and Intra-Host Genetic Evolution of Zika Virus Infection in Symptomatic Adults: A Special View in the Male Reproductive System. Viruses 10 (11), 615.

Onorati, M., Li, Z., Liu, F., Sousa, A.M., Nakagawa, N., Li, M., Dell'Anno, M., Gulden, F., Pochareddy, S., Tebbenkamp, A.N., Han, W., Pletikos, M., Gao, T., Zhu, Y., Bichsel, C., Varela, L., Szigeti-Buck, K., Lisgo, S., Zhang, Y., Testen, A., Gao, X.-B., Mlakar, J., Popovic, M., Flamand, M., Strittmatter, S., Kaczmarek, L., Anton, E.S., Horvath, T., Lindenbach, B., Sestan, N., 2016. Zika Virus Disrupts Phospho-TBK1 Localization and Mitosis in Human Neuroepithelial Stem Cells and Radial Glia. Cell Rep. 16 (10), 2576–2592.

Panganiban, A.T., Blair, R.V., Hattler, J.B., Bohannon, D.G., Bonaldo, M.C., Schouest, B., Maness, N.J., Kim, W.-K., 2020. A Zika virus primary isolate induces neuroinflammation, compromises the blood-brain barrier and upregulates CXCL12 in adult macaques. Brain Pathology (Zurich, Switzerland) 30 (6), 1017–1027.

Patel, R.T., Gallamoza, B.M., Kulkarni, P., Sherer, M.L., Haas, N.A., Lemanski, E., Malik, I., Hekmatyar, K., Parcells, M.S., Schwarz, J.M., 2021. An examination of the long-term neurodevelopmental impact of prenatal zika virus infection in a rat model using a high resolution, longitudinal mri approach. Viruses 13 (6). https://doi.org/10.3390/V13061123/S1.

Pun, P.B.L., Lu, J., Moochhala, S., 2009. Involvement of ROS in BBB dysfunction. Free Radic. Res. 43 (4), 348–364. https://doi.org/10.1080/10715760902751902.

Sanches, E. F., Arteni, N. S., Spindler, C., Moyses, F., Siqueira, I. R., Perry, M. L., & Netto, C. A. (2012). Effects of pre- and postnatal protein malnutrition in hypoxic-ischemic rats. *Brain Res*, *1438*, 85–92. https://doi.org/S0006-8993(11)02225-6 [pii] 10.1016/j.brainres.2011.12.024.

Sanches, E. F., Arteni, N. S., Spindler, C., Moysés, F., Siqueira, I. R., Perry, M. L., Netto, C. A., Moyses, F., Siqueira, I. R., Perry, M. L., & Netto, C. A. (2012). Effects of pre- and postnatal protein malnutrition in hypoxic-ischemic rats. *Brain Res*, *1438*, 85–92. https://doi.org/S0006-8993(11)02225-6 [pii] 10.1016/j.brainres.2011.12.024.

Sandler, A.D., Brazdziunas, D., Cooley, W.C., González De Pijem, L., Hirsch, D., Kastner, T.A., Kummer, M.E., Quint, R.D., Ruppert, E.S., Anderson, W.C., Crider, B., Burgan, P., Garner, C., McPherson, M., Michaud, L., Yeargin-Allsopp, M., Cartwright, J.D., Johnson, C.P., Smith, K., 2001. Developmental Surveillance and Screening of Infants and Young Children. Pediatrics 108 (1), 192–195. https://doi.org/10.1542/PEDS.108.1.192.

Sasso, S., Dalmedico, L., Magro, D.D., Pereira, E.M., Wyse, A.T., de Lima, D.D., 2015. Differential in vitro effects of homoarginine on oxidative stress in plasma, erythrocytes, kidney and liver of rats in the absence and in the presence alpha-tocopherol, ascorbic acid or L-NAME. Amino Acids 47 (9), 1931–1939. https://doi.org/10.1007/s00726-015-1973-6.

Schuch, C.P., Diaz, R., Deckmann, I., Rojas, J.J., Deniz, B.F., Pereira, L.O., 2016. Early environmental enrichment affects neurobehavioral development and prevents brain damage in rats submitted to neonatal hypoxia-ischemia. Neurosci. Lett. 617, 101–107. https://doi.org/10.1016/j.neulet.2016.02.015.

Schweinberger, B.M., Turcatel, E., Rodrigues, A.F., Wyse, A.T., 2015. Gestational hypermethioninaemia alters oxidative/nitrative status in skeletal muscle and biomarkers of muscular injury and inflammation in serum of rat offspring. Int. J. Exp. Pathol. 96 (5), 277–284. https://doi.org/10.1111/iep.12136.

Semple, B.D., Blomgren, K., Gimlin, K., Ferriero, D.M., Noble-Haeusslein, L.J., 2013. Brain development in rodents and humans: Identifying benchmarks of maturation and vulnerability to injury across species. Prog. Neurobiol. 106-107, 1–16.

Shapiro-Mendoza, C.K., Rice, M.E., Galang, R.R., Fulton, A.C., VanMaldeghem, K., Prado, M.V., Ellis, E., Anesi, M.S., Simeone, R.M., Petersen, E.E., Ellington, S.R., Jones, A.M., Williams, T., Reagan-Steiner, S., Perez-Padilla, J., Deseda, C.C., Beron, A., Tufa, A.J., Rosinger, A., Roth, N.M., Green, C., Martin, S., Lopez, C.D., deWilde, L., Goodwin, M., Pagano, H.P., Mai, C.T., Gould, C., Zaki, S., Ferrer, L.N., Davis, M.S., Lathrop, E., Polen, K., Cragan, J.D., Reynolds, M., Newsome, K.B., Huertas, M.M., Bhatangar, J., Quiñones, A.M., Nahabedian, J.F., Adams, L., Sharp, T. M., Hancock, W.T., Rasmussen, S.A., Moore, C.A., Jamieson, D.J., Munoz-Jordan, J. L., Garstang, H., Kambui, A., Masao, C., Honein, M.A., Meaney-Delman, D., Rico, A., Phippard, A., Peterson, A.B., Pomales, A., Arth, A.C., Dawson, A., Rey, A., Figueroa, A., Sanchez, A., Robinson, B., Williams, D.B., Dee, D.L., Forbes, D.P., Ailes, E.C., Marrero, F., Fortenberry, G.Z., Razzaghi, H., Ko, J.Y., Lind, J.N., Dominguez, K.L., Clarke, K., Flores, M., Biggerstaff, M.S., Danielson, M., Molina, M., Somerville, N.J., Blumenfeld, R., Tuff, R.A., Free, R.J., Chae, S.-R., Andrist, S., Kim, S.Y., Williams, T.L., Harrington, T.A., Thomason, T., Krishnasamy, V., 2017. Pregnancy Outcomes After Maternal Zika Virus Infection During Pregnancy — U.S. Territories, January 1, 2016–April 25, 2017. MMWR Morb. Mortal. Wkly Rep. 66 (23), 615–621.

Sherer, M.L., Khanal, P., Talham, G., Brannick, E.M., Parcells, M.S., Schwarz, J.M., Biagini, G., 2019. Zika virus infection of pregnant rats and associated neurological consequences in the offspring. PLoS One 14 (6), e0218539.

Sherer, M.L., Lemanski, E.A., Patel, R.T., Wheeler, S.R., Parcells, M.S., Schwarz, J.M., 2021. A Rat Model of Prenatal Zika Virus Infection and Associated Long-Term Outcomes. Viruses 13 (11). https://doi.org/10.3390/V13112298.

Smirnov, K., Sitnikova, E., 2019. Developmental milestones and behavior of infant rats: The role of sensory input from whiskers. Behav. Brain Res. 374, 112143 https://doi.org/10.1016/J.BBR.2019.112143.

Snyder-Keller, A., Kramer, L.D., Zink, S., Bolivar, V.J., 2019. Mouse Strain and Sex-Dependent Differences in Long-term Behavioral Abnormalities and Neuropathologies after Developmental Zika Infection. J. Neurosci. 39 (27), 5393–5403. https://doi.org/10.1523/JNEUROSCI.2666-18.2019.

Sobral da Silva, P. F., Eickmann, S. H., Ximenes, R. A. de A., Martelli, C. M. T., Brickley, E. B., Lima, M. C., Montarroyos, U. R., de Carvalho, M. D. C. G., Rodrigues, L. C., de Araújo, T. V. B., Ventura, L. O., Oliveira, D. M. da S., Ramos, R. C. F., & Miranda-Filho, D. de B. (2021). Neurodevelopment in Children Exposed to Zika Virus: What Are the Consequences for Children Who Do Not Present with Microcephaly at Birth? *Viruses*, *13*(8). https://doi.org/10.3390/V13081427.

Song, B.H., Yun, S.I., Woolley, M., Lee, Y.M., 2017. Zika virus: History, epidemiology, transmission, and clinical presentation. J. Neuroimmunol. 308, 50–64. https://doi.org/10.1016/J.JNEUROIM.2017.03.001.

Stanelle-Bertram, S., Walendy-Gnirß, K., Speiseder, T., Thiele, S., Asante, I.A., Dreier, C., Kouassi, N.M., Preuß, A., Pilnitz-Stolze, G., Müller, U., Thanisch, S., Richter, M., Scharrenberg, R., Kraus, V., Dörk, R., Schau, L., Herder, V., Gerhauser, I., Pfankuche, V.M., Käufer, C., Waltl, I., Moraes, T., Sellau, J., Hoenow, S., Schmidt-Chanasit, J., Jansen, S., Schattling, B., Ittrich, H., Bartsch, U., Renné, T., Bartenschlager, R., Arck, P., Cadar, D., Friese, M.A., Vapalahti, O., Lotter, H., Benites, S., Rolling, L., Gabriel, M., Baumgärtner, W., Morellini, F., Hölter, S.M., Amarie, O., Fuchs, H., Hrabe de Angelis, M., Löscher, W., Calderon de Anda, F., Gabriel, G., 2018. Male offspring born to mildly ZIKV-infected mice are at risk of developing neurocognitive disorders in adulthood. Nat. Microbiol. 3 (10), 1161–1174.

Tang, H., Hammack, C., Ogden, S.C., Wen, Z., Qian, X., Li, Y., Yao, B., Shin, J., Zhang, F., Lee, E.M., Christian, K.M., Didier, R.A., Jin, P., Song, H., Ming, G.L., 2016. Zika Virus Infects Human Cortical Neural Progenitors and Attenuates Their Growth. Cell Stem Cell 18 (5), 587–590. https://doi.org/10.1016/J.STEM.2016.02.016.

Vue, D., & Tang, Q. (2021). Zika Virus Overview: Transmission, Origin, Pathogenesis, Animal Model and Diagnosis. *Zoonoses (Burlington, Mass.)*, *1*(1). https://doi.org/10.15212/ZOONOSES-2021-0017.

Wachholz, G.E., Varela, A.P.M., Teixeira, T.F., de Matos, S.M.S., da Luz, R., Soster, P., Vianna, F.S.L., de Souza, D.O.G., Roehe, P.M., Schuler-Faccini, L., Fraga, L.R., 2021. Zika virus-induced brain malformations in chicken embryos. Birth Defects Res. 113 (1), 22–31. https://doi.org/10.1002/BDR2.1813.

Wang, J.N., Ling, F., 2016. Zika Virus Infection and Microcephaly: Evidence for a Causal Link. Int. J. Environ. Res. Public Health 13 (10). https://doi.org/10.3390/IJERPH13101031.